Prolonged Injury and Altered Lung Function after Ozone Inhalation in Mice with Chronic Lung Inflammation

Angela M. Groves[1], Andrew J. Gow[1], Christopher B. Massa[1], Jeffrey D. Laskin[2], and Debra L. Laskin[1]

[1]Department of Pharmacology and Toxicology, Ernest Mario School of Pharmacy, Rutgers University, Piscataway, New Jersey; and [2]Department of Environmental and Occupational Medicine, Robert Wood Johnson Medical School, University of Medicine and Dentistry of New Jersey, Piscataway, New Jersey

Surfactant protein–D (Sftpd) is a pulmonary collectin important in down-regulating macrophage inflammatory responses. In these experiments, we analyzed the effects of chronic macrophage inflammation attributable to loss of *Sftpd* on the persistence of ozone-induced injury, macrophage activation, and altered functioning in the lung. Wild-type (*Sftpd*$^{+/+}$) and *Sftpd*$^{-/-}$ mice (aged 8 wk) were exposed to air or ozone (0.8 parts per million, 3 h). Bronchoalveolar lavage (BAL) fluid and tissue were collected 72 hours later. In *Sftpd*$^{-/-}$ mice, but not *Sftpd*$^{+/+}$ mice, increased BAL protein and nitrogen oxides were observed after ozone inhalation, indicating prolonged lung injury and oxidative stress. Increased numbers of macrophages were also present in BAL fluid and in histologic sections from *Sftpd*$^{-/-}$ mice. These cells were enlarged and foamy, suggesting that they were activated. This conclusion was supported by findings of increased BAL chemotactic activity, and increased expression of inducible nitric oxide synthase in lung macrophages. In both *Sftpd*$^{+/+}$ and *Sftpd*$^{-/-}$ mice, inhalation of ozone was associated with functional alterations in the lung. Although these alterations were limited to central airway mechanics in *Sftpd*$^{+/+}$ mice, both central airway and parenchymal mechanics were modified by ozone exposure in *Sftpd*$^{-/-}$ mice. The most notable changes were evident in resistance and elastance spectra and baseline lung function, and in lung responsiveness to changes in positive end-expiratory pressure. These data demonstrate that a loss of *Sftpd* is associated with prolonged lung injury, oxidative stress, and macrophage accumulation and activation in response to ozone, and with more extensive functional changes consistent with the loss of parenchymal integrity.

Keywords: ozone; surfactant protein–D; macrophages; iNOS; lung function

CLINICAL RELEVANCE

Chronic inflammation is a characteristic feature of such lung diseases as chronic obstructive pulmonary disease and asthma. The present study demonstrates that ozone-induced lung injury, oxidative stress, and macrophage activation are prolonged in a murine model of persistent pulmonary macrophage inflammation. Furthermore, this prolonged activation is associated with exacerbations of functional defects in pulmonary mechanics. These results may be important for understanding the response of individuals with preexisting inflammatory lung disease to urban air pollutants.

Ozone is a ubiquitous urban air pollutant generated as a component of photochemical smog. Inhaled ozone causes ozonation and the peroxidation of proteins and lipids in the epithelial lining fluid layer of the lung, resulting in the production of oxidized proteins, aldehydes, and free radicals, which can damage surrounding tissue (1, 2). This is accompanied by an accumulation of activated macrophages in the lung and the production of additional cytotoxic and proinflammatory mediators, including reactive oxygen and reactive nitrogen species (ROS and RNS, respectively) that contribute to tissue injury (3). Airway and tissue mechanics are also altered after ozone exposure. Thus, in humans, ozone inhalation leads to a deterioration of pulmonary function, as measured by decreases in respiratory frequency, forced expiratory volume in 1 second, and forced vital capacity, and increases in airway resistance (1, 4, 5). Ozone has been shown to exacerbate asthma and increase airway hyperreactivity (5, 6), and to contribute to increased morbidity and mortality in patients with chronic obstructive pulmonary disease (COPD) (7, 8). Similar alterations in lung function and increases in sensitivity to ozone have been described in animal models of asthma and allergic inflammation (9–11).

Surfactant protein–D (Sftpd) is a pulmonary collectin synthesized mainly by alveolar Type II cells, and it plays a key role in innate immune defense (12, 13). Under homeostatic conditions, Sftpd functions as an anti-inflammatory protein, in part by suppressing NF-κB–mediated transcription of inflammatory genes (14). However, after the induction of oxidative stress, modification of critical cysteines in Sftpd by reactive species such as nitric oxide leads to a change in its activity to a proinflammatory mediator (15). Findings of persistent localization of macrophages in the lung and increased production of ROS and RNS by these cells in mice lacking native *Sftpd* are consistent with its anti-inflammatory function (16, 17). In previous studies, we demonstrated that inflammatory macrophages and mediators they release play key roles in lung injury and oxidative stress induced by ozone (3, 18, 19). Based on these observations, we hypothesized that persistent macrophage localization and activation in the lung as a result of the loss of *Sftpd* would result in a prolonged sensitivity of mice to inhaled ozone. Moreover, this sensitivity would be associated with exacerbated functional defects in the lung. To test this hypothesis, we analyzed the effects of ozone on lung injury, oxidative stress, macrophage activation, and pulmonary mechanics in *Sftpd*$^{-/-}$ mice 72 hours after exposure, a time when inflammation and injury have, for the most part,

(*Received in original form December 14, 2011 and in final form July 30, 2012*)

This research was supported by National Institute of Health grants R01ES004738, R01CA132624, R01GM034310, R01HL086621, U54AR055073, P30ES005022, and T32ES007148 (D.L.L.).

Correspondence and requests for reprints should be addressed to Debra L. Laskin, Ph.D., Department of Pharmacology and Toxicology, Ernest Mario School of Pharmacy, Rutgers University, 160 Frelinghuysen Road, Piscataway, NJ 08854. E-mail: laskin@eohsi.rutgers.edu

This article has an online supplement, which is accessible from this issue's table of contents at www.atsjournals.org

Am J Respir Cell Mol Biol Vol 47, Iss. 6, pp 776–783, Dec 2012

Originally Published in Press as DOI: 10.1165/rcmb.2011-0433OC on August 9, 2012
Internet address: www.atsjournals.org

resolved in wild-type mice (18). We also developed a novel experimental modeling approach to analyze alterations in lung function, with the goals of dissecting the effects of ozone on central airways and parenchyma, and of assessing heterogeneity in lung responsiveness and the propensity for alterations in lung stiffness. The results of our studies, along with previous reports of increases in lung neutrophils in *Sftpd*$^{-/-}$ mice after ozone exposure (13), highlight the importance of analyzing underlying disease pathology in susceptibility to pulmonary irritants.

MATERIALS AND METHODS

Animals and Exposures

Male C57Bl/6J wild-type (*Sftpd*$^{+/+}$) mice (8 wk of age) were purchased from the Jackson Laboratories (Bar Harbor, ME). *Sftpd*$^{-/-}$ mice were generated on a C57Bl/6 background (20) and were bred at Rutgers University. Animals were housed in microisolation cages and received food and water *ad libitum*. Mice were killed 72 hours after exposure (for 3 h) to ozone (0.8 parts per million) or air in whole-body Plexiglas chambers. Ozone was generated using a Gilmont generator (Orec, Phoenix, AZ). Concentrations in the chamber were monitored using a Teledyne ozone analyzer (Teledyne, Thousand Oaks, CA). Bronchoalveolar lavage (BAL) cell and protein content, nitrogen oxides (NOx), and chemotactic activity were assayed as previously described (15, 17, 18) and in the online supplement.

Histology and Immunohistochemistry

Tissues sections (6 μm) were stained with hematoxylin and eosin, and scored blindly by two independent observers for severity of inflammation in peribronchiolar and perivascular regions of the lung on a scale of 0 (no inflammation) to 5 (severe inflammation) (21). Immunohistochemistry was performed according to our previous work (22).

Measurement of Pulmonary Mechanics

Respiratory mechanics were measured using a FlexiVent (SCIREQ, Montreal, PQ, Canada) at positive end-expiratory pressures (PEEPs) ranging from 0–6 cm H_2O (23). Parameters of dynamic whole-lung mechanics, including total dynamic resistance (R) and compliance (C), were determined from a single-compartment model by multiple linear regressions. Lung function measurements were also partitioned into parameters representing the properties of the airways or the parenchyma by analyzing input impedance data (Z_L), generated using an 8-second broadband flow perturbation. Data from the impedance spectra were fit to a constant phase model, allowing for the calculation of frequency-independent central airway resistance (Rn) and the coefficients of tissue damping (G) and tissue elastance (H) in the tissue compartment (24). Hysteresivity (η) was calculated from the ratio of G/H. A pressure volume curve was generated and used to calculate static compliance (Cst) (*see* the online supplement for further details). Resistance and elastance spectra were generated from Z_L. To characterize Z_L spectra with higher fidelity, best fit lines were generated using nonlinear regression analysis. Parameters representing key features of the resistance spectra curve (R_L) were calculated as:

$$R_L = (a + bf)/(c + f),$$

where f = frequency, a/c = the low-frequency asymptote of the curve when tissue resistive and viscous effects predominate, and b = the high-frequency asymptote, when airway resistive effects predominate. Parameters representing different portions of the elastance spectra curve (E_L) were calculated as:

$$E_L = E_0 + \Delta E\left(1 - e^{-\beta f}\right),$$

where $E_0 = E_L$ at 0 Hz, representing the portion of the E_L at low frequencies, and reflecting intrinsic tissue stiffness, ΔE = the magnitude of E_L, and β = the rate E_L changes with frequency.

Statistical Analysis

All experiments were repeated three times. Data were analyzed by two-way ANOVA and a nonpaired two-tailed Student *t* test, or nonparametrically using a Mann-Whitney rank sum test. R_L and E_L spectra were analyzed using nonlinear regression (*see* the online supplement for further details).

RESULTS

Effects of Ozone Inhalation on Lung Injury and Macrophage Activation in *Sftpd*$^{+/+}$ and *Sftpd*$^{-/-}$ Mice

Consistent with previous work (18), we found that ozone-induced lung injury, inflammation, and oxidative stress, which are prominent at 24 hours and 48 hours after exposure, had for the most part resolved by 72 hours (Figure 1). Thus, no significant differences were evident between air-exposed and ozone-exposed *Sftpd*$^{+/+}$ mice in BAL cell number, composition (> 99.7% macrophages), protein, or NOx concentrations. Similarly, ozone exposure exerted no effect on BAL chemotactic activity, which we previously demonstrated correlates with lung inflammatory cell activity (15), or on lung inflammation scores (Figures 1 and 2). Inactivation of the *Sftpd* gene results in the development of persistent pulmonary inflammation, characterized by a predominant macrophage infiltrate, which progresses to emphysema as the animal becomes older (20, 25). In further experiments, we examined whether this change in baseline inflammation, before the development of emphysema (Figure E1 in the online supplement), alters the response of mice to ozone. Loss of *Sftpd* by itself exerted no significant effect on lung injury, oxidative stress, or inflammatory cell activation, as measured by BAL protein, NOx, and chemotactic activity (Figure 1). In contrast, BAL cell number was increased in *Sftpd*$^{-/-}$ mice relative to *Sftpd*$^{+/+}$ mice. The majority of these cells (> 99.5%) were macrophages (Figure 1). Inflammation scores were also higher in *Sftpd*$^{-/-}$ mice (Figure 2). In *Sftpd*$^{-/-}$ mice, ozone exposure resulted in a threefold increase in the number of cells recovered in BAL fluid (Figure 1). This was associated with a twofold increase in inflammation scores (Figure 2). Lung lavage exerted no effect on inflammation scores or on the accumulation of these cells in tissue (Figure E2 in the online supplement). In air-exposed *Sftpd*$^{-/-}$ mice, but not *Sftpd*$^{+/+}$ mice, we also noted a peribronchial accumulation of enlarged foamy macrophages. This accumulation became more pronounced after ozone exposure. BAL macrophage numbers, protein and NOx concentrations, and BAL chemotactic activity, were also significantly increased in *Sftpd*$^{-/-}$ mice after exposure to ozone (Figure 1). Ozone-induced increases in lung inflammation, as assessed by BAL cell number, persisted for at least 96 hours in *Sftpd*$^{-/-}$ mice (not shown).

We next assessed the expression of inducible nitric oxide synthase (iNOS) and cyclooxygenase-2 (COX-2), enzymes important in the generation of proinflammatory RNS and eicosanoids, respectively, and markers of classically activated macrophages (26–29). Low levels of iNOS and COX-2 protein expression were evident in the lungs of *Sftpd*$^{-/-}$ mice, but not *Sftpd*$^{+/+}$ mice (Figure 3). Whereas iNOS was localized in alveolar macrophages, COX-2 was mainly localized in Type II cells. In *Sftpd*$^{+/+}$ mice, ozone exposure resulted in increased expression of COX-2 in Type II cells, with no effect on iNOS (*see* Figure E3 in the online supplement for quantitation). In contrast, in *Sftpd*$^{-/-}$ mice treated with ozone, increases in the expression of iNOS in macrophages and of COX-2 in Type II cells were evident.

Effects of Ozone Inhalation on Lung Function in *Sftpd*$^{+/+}$ and *Sftpd*$^{-/-}$ Mice

To examine the physiological consequences of ozone-induced injury in *Sftpd*$^{-/-}$ mice, we measured lung function using a series

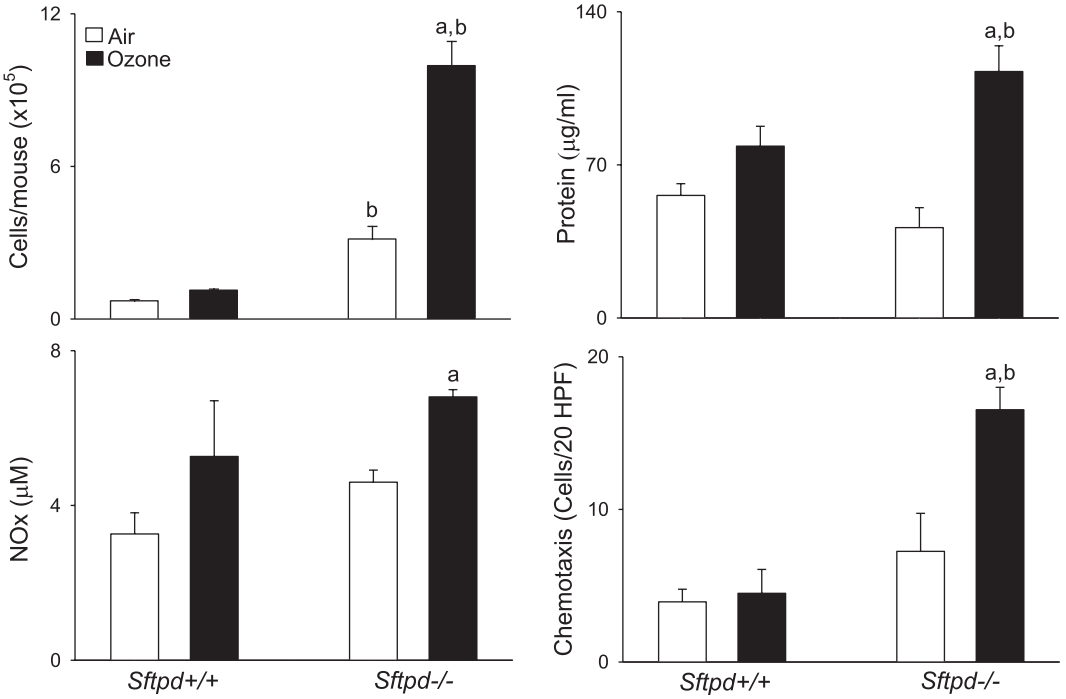

Figure 1. Effects of ozone inhalation on lung inflammation and injury. Bronchoalveolar lavage (BAL) was collected 72 hours after exposure of *Sftpd*$^{+/+}$ and *Sftpd*$^{-/-}$ mice to air or ozone and analyzed for cell, protein, and nitrogen oxides (NOx) content, and for chemotactic activity. BAL chemotactic activity was assessed using the RAW 264.7 murine macrophage cell line (American Type Culture Collection, Manassas, VA), as previously described (15). Hanks' balanced salt solution was used as the negative control. Chemotaxis data are expressed as the average number of migrated cells per 20 high-power fields (HPF). The value range for these experiments was 0–30 migrated cells per high power field. Each bar represents the mean ± SEM of three experiments (n = 4–9 mice/treatment group/experiment; n = 12–27 mice/group total). Data were analyzed by two-way ANOVA. [a]Significantly different ($P \leq 0.05$) from air-exposed control mice. [b]Significantly different ($P \leq 0.05$) from *Sftpd*$^{+/+}$ mice. Sftpd, surfactant protein–D.

of perturbations including single-frequency and broadband forced oscillation, pressure–volume loops, and lung volume measurements. Initially, respiratory mechanics were partitioned into airway and tissue responses by analyzing impedance spectra data, using a constant phase model (24). At baseline, R, Rn, and Cst values were greater in *Sftpd*$^{-/-}$ mice, compared with *Sftpd*$^{+/+}$ mice (Table 1). In *Sftpd*$^{+/+}$ mice, ozone inhalation resulted in increased Rn, relative to air-exposed control mice, whereas in *Sftpd*$^{-/-}$ mice, significant changes were only observed in H and Cst (Table 1). We also measured η and G; neither of these parameters was altered by the loss of *Sftpd* or by ozone inhalation (data not shown).

The effects of altering PEEP on lung function were next evaluated, to allow for the assessment of heterogeneity in responsiveness and changes in airway/parenchymal elastic properties (30). In *Sftpd*$^{+/+}$ mice, increasing PEEP from 3 to 6 cm H_2O resulted in increases of both Rn and Cst (Figure 4). Similar changes were observed in *Sftpd*$^{-/-}$ mice. However, the PEEP-dependent increase in Rn was blunted relative to *Sftpd*$^{+/+}$ mice. Treatment of mice with ozone exerted no major effects on Cst at any of the PEEPs examined (Figure 4). In contrast, after ozone exposure, both *Sftpd*$^{+/+}$ and *Sftpd*$^{-/-}$ mice were significantly less responsive to increasing PEEP from 3 to 6 cm H_2O with respect to Rn, although they were more responsive to PEEPs below 3 cm H_2O.

In further experiments, we examined the effects of changes in PEEP on the R_L and E_L spectra derived directly from the forced oscillation technique, which more accurately reflects heterogeneous lung injury (31). Ozone exposure produced no significant changes in the overall R_L spectra in *Sftpd*$^{+/+}$ mice, whereas a frequency-dependent increase in E_L spectra was observed at PEEPs of 0 and 1 cm H_2O (Figure 5). E_L spectra were also significantly increased in ozone-exposed *Sftpd*$^{-/-}$ mice, relative to air-exposed animals. However, this response was observed at all PEEP levels. In *Sftpd*$^{-/-}$ mice, increases in R_L spectra were also observed at a PEEP of 0 cm H_2O after ozone exposure. Changes in R_L were most evident at low frequencies. To ensure that lung volume–related changes did not influence analyses of R_L and E_L spectra, initial lung volumes were established at 0 PEEP. No significant differences were evident between groups (Table E1 in the online supplement).

To better quantify changes in the resistive and elastic properties of the lung after ozone exposure, R_L and E_L spectra were fit to model equations, such that the parameters defining these responses could be estimated (*see* MATERIALS AND METHODS and the online supplement). In *Sftpd*$^{+/+}$ mice, ozone exposure produced no significant change in a, whereas b was significantly increased at 1 cm and 3 cm H_2O, and c decreased at 6 cm H_2O, when compared with air-exposed mice (Table 2). A significant increase in ΔE, accompanied by a fall in β, was observed at low PEEPs after the exposure of *Sftpd*$^{+/+}$ mice to ozone, with no effect on inherent elastance (E_0). The loss of *Sftpd* resulted in a different pattern of changes in these parameters in response to ozone. Thus, at low PEEPs, a increased significantly in *Sftpd*$^{-/-}$ mice after ozone inhalation, whereas b decreased. In contrast, c was not altered at any PEEP examined. In *Sftpd*$^{-/-}$ mice, ozone inhalation also produced a significant increase in inherent elastance, as shown by elevated E_0 at all PEEPs. In addition, at low PEEPs, ozone exposure resulted in increased ΔE and decreased β, indicating a high-frequency, ventilation-dependent increase in lung stiffness.

In air-exposed *Sftpd*$^{-/-}$ mice, no significant changes in a were evident across all PEEPs when compared with *Sftpd*$^{+/+}$ mice (Table 2). However, the loss of *Sftpd* did result in a significant elevation of b at all PEEPs, whereas at high PEEPs, a significant decrease in c was observed. No significant changes in ΔE were evident in mice lacking *Sftpd* at any level of PEEP. However, E_0 was decreased at low PEEPs. In contrast, the loss of *Sftpd* resulted in a significant increase in β at a PEEP of 6 cm H_2O.

DISCUSSION

Accumulating evidence suggests that lung injury induced by ozone is a result of its direct interaction with proteins and lipids in the epithelial lining fluid, and of the actions of ROS, RNS, and

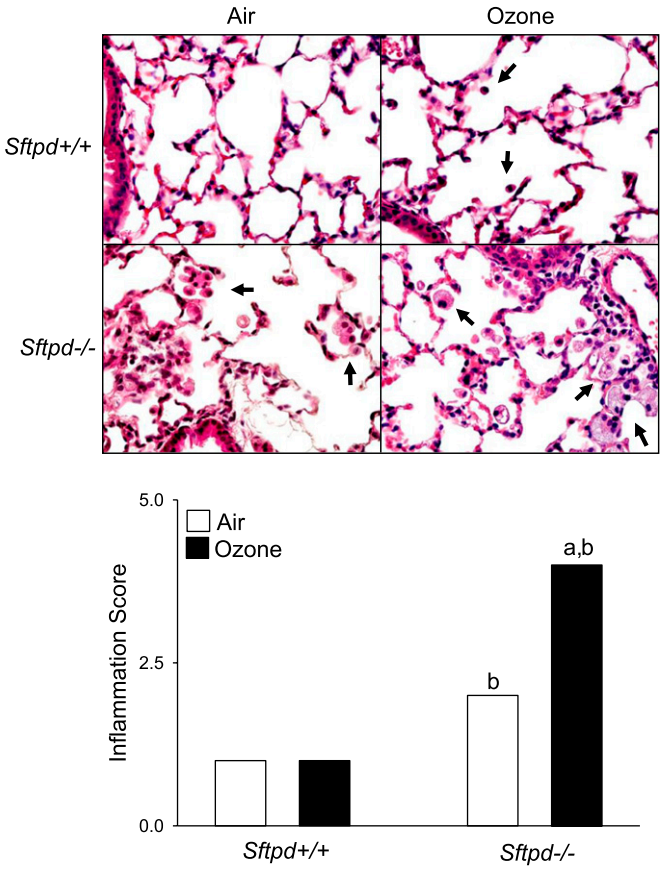

Figure 2. Effects of ozone inhalation on lung structure and inflammation score. *Top*: Lung sections, prepared 72 hours after exposure of *Sftpd*$^{+/+}$ and *Sftpd*$^{-/-}$ mice to air or ozone, were stained with hematoxylin and eosin. *Arrows* indicate alveolar macrophages. *Original magnification*, ×600. *Bottom*: Slides were scored blindly by two independent observers for severity of inflammation on a scale of 0–5 (0, no inflammation; 5, severe inflammation). Each bar represents the median of three experiments ($n = 4$–9 mice/treatment group/experiment; $n = 12$–27 mice/group total). Significance was assessed by ANOVA, based on ranks. [a]Significantly different ($P \leq 0.05$) from air-exposed control mice. [b]Significantly different ($P \leq 0.05$) from *Sftpd*$^{+/+}$ mice.

other cytotoxic mediators generated by inflammatory cells (1–3). Sftpd plays a key role in regulating inflammatory responses in the lung. Specifically, it acts to balance macrophage activation in a manner dependent upon modifications by nitric oxide (13–15). In the absence of *Sftpd*, mice develop progressive inflammatory disease in the lung, characterized by a predominant peribronchiolar macrophage infiltrate, airspace enlargement, and increases in lung volume, culminating in emphysema (25). The present experiments demonstrate that the persistent localization of activated macrophages in the lung, associated with a loss of *Sftpd*, results in the prolonged sensitivity of mice to the cytotoxic effects of inhaled ozone, and causes exacerbated alterations in lung function. These data are novel and provide support for a critical protective role of Sftpd in regulating macrophage inflammatory responses and oxidative stress within the lung (14, 15, 17).

Previous studies from our laboratory demonstrated that ozone-induced inflammation, as measured by numbers of alveolar macrophages recovered in BAL, peaks 48 hours after acute exposure, returning to control levels by 72 hours (18). Consistent with these results, the present experiments show that BAL macrophage numbers and chemotactic activity, as well as lung inflammation scores, were at control levels 72 hours after exposure of *Sftpd*$^{+/+}$ mice to ozone. The observation that BAL NOx and protein concentrations were also similar in air-exposed and ozone-exposed *Sftpd*$^{+/+}$ mice indicates that oxidative stress and alveolar epithelial barrier dysfunction have also resolved by this time. Despite the resolution of these responses, *Sftpd*$^{+/+}$ mice remain functionally compromised 72 hours after ozone inhalation. Thus, in these mice, Rn was significantly increased, with no apparent effect on the parenchyma, as measured by H and G. These findings are in accordance with reports of hyperreactivity in response to methacholine challenge after ozone exposure (4, 32). Interestingly, at PEEPs both above and below the physiological level of 3 cm H_2O, which represent hypoinflation and hyperinflation of the lung, respectively, a decrease in Rn was evident after ozone exposure. This observation, however, was not consistent with the lack of change in H and G, because it implies that parenchymal recruitment affects Rn. We speculated that these differences may be attributed to the use of a constant phase model to analyze our data, which assumes that the lung behaves homogeneously in terms of both its resistive and elastic properties. Therefore, to take into account heterogeneity in the response of the lung to ozone, impedance frequency spectra were analyzed. Because different portions of the impedance frequency spectrum represent distinct components of the respiratory system, effects on airway and parenchymal components can readily be distinguished

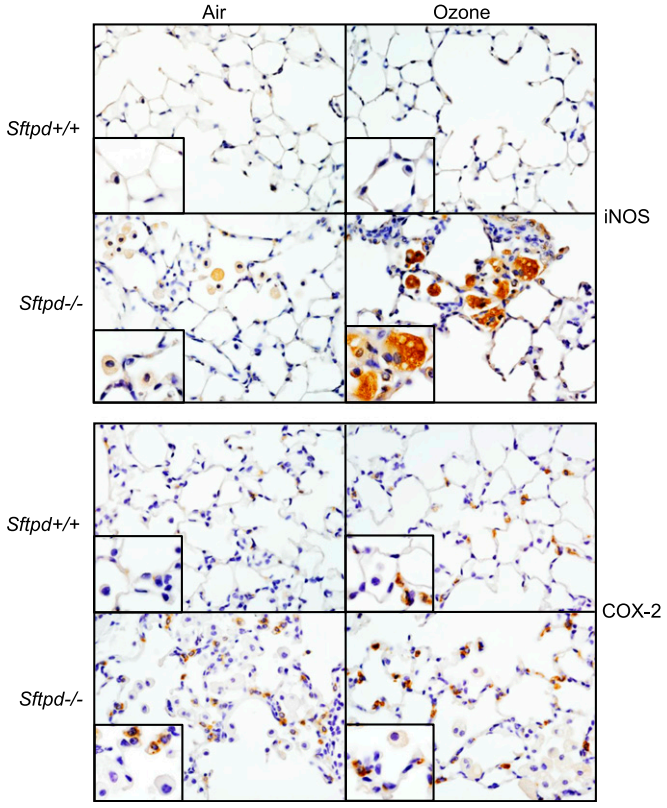

Figure 3. Effects of ozone inhalation on lung expression of inducible nitric oxide synthase (iNOS) and cyclooxygenase-2 (COX-2). Lung sections, prepared 72 hours after exposure of *Sftpd*$^{+/+}$ and *Sftpd*$^{-/-}$ mice to air or ozone, were stained with a 1:100 dilution of antibody to iNOS (*above*), a 1:1,000 dilution of antibody to COX-2 (*below*), or IgG control, followed by a 1:200 dilution of biotinylated secondary antibody. Binding was visualized using a peroxidase substrate DAB kit (Vector Laboratories, Burlingame, CA). *Insets* show iNOS-positive or COX-2–positive cells. One representative section is shown from three separate experiments ($n = 3$ mice/treatment group/experiment). *Original magnification*, ×600; *inset*, ×1,000.

TABLE 1. EFFECTS OF OZONE ON BASELINE LUNG FUNCTION IN *SFTPD*$^{+/+}$ AND *SFTPD*$^{-/-}$ MICE

	Sftpd$^{+/+}$		*Sftpd*$^{-/-}$	
	Air	Ozone	Air	Ozone
R (cm H_2O · s/ml)	0.97 ± 0.03	1.08 ± 0.03	1.37 ± 0.05*	1.35 ± 0.11*
Rn (mm H_2O · s/ml)	24.42 ± 1.0	44.83 ± 2.2†	49.39 ± 2.2*	46.60 ± 1.3
C (ml/mm H_2O)	1.88 ± 0.0	1.79 ± 0.1	1.84 ± 0.1	1.51 ± 0.1*
Cst (ml/mm H_2O)	2.84 ± 0.1	2.78 ± 0.1	3.33 ± 0.2*	2.53 ± 0.2[a]
H (cm H_2O/ml)	56.44 ± 1.51	59.48 ± 2.34	53.15 ± 3.38	65.24 ± 3.73†

Definition of abbreviations: C, compliance; Cst, static compliance; H, tissue elastance; R, dynamic resistance; Rn, central airway resistance; Sftpd, surfactant protein–D.

Lung function was measured 72 hours after exposure of *Sftpd*$^{+/+}$ and *Sftpd*$^{-/-}$ mice to air or ozone at a PEEP of 3 cm H_2O. Each measurement was performed in triplicate. Values represent the means ± SEM of three experiments (n = 4–6 mice/treatment group/experiment; n = 12–18 mice/group total). Data were analyzed by two-way ANOVA.

* Significantly different ($P < 0.05$) from *Sftpd*$^{+/+}$ mice.

† Significantly different ($P < 0.05$) from air-exposed control mice.

(33). Whereas the resistance (R_L) spectra were not significantly altered in ozone-exposed mice, when compared with air-exposed mice, significant changes in the component parameters a, b, and c were evident. The nature of these changes indicated that with full recruitment and hyperinflation, a reduction in the low-frequency component of the R_L spectrum occurs after ozone exposure, supporting the idea that ozone causes a loss of parenchymal integrity. Consistent with this conclusion are our findings that at low PEEPs, ozone inhalation significantly altered the elastance (E_L) spectra in *Sftpd*$^{+/+}$ mice. To analyze this alteration, E_L spectra data were fit to a three-parameter exponential model (*see* MATERIALS AND METHODS). Our observation that ozone exerted no effect on any of the parameters at a physiological PEEP of 3 cm H_2O is in agreement with the constant phase model. In contrast, low PEEP spectra showed a lung recruitment/frequency-dependent change in the elastic properties of the lung after ozone exposure. These data, together with the changes observed in R_L spectra, indicate a loss of parenchymal tethering resulting in a failure to maintain airway patency at low PEEPs, and as the lung inflates (at high PEEP), a loss of lung stiffness. This approach to analyzing functional alterations in the lung is novel and provides new insights into the heterogeneous nature of tissue injury induced by ozone.

In accord with previous reports (17, 20), we found that mice lacking *Sftpd* exhibited significant pulmonary inflammation relative to *Sftpd*$^{+/+}$ mice, characterized by increased numbers of macrophages in the lung and in BAL fluid. We also observed that lung macrophages were enlarged in *Sftpd*$^{-/-}$ mice relative to *Sftpd*$^{+/+}$ mice, and exhibited a foamy appearance, suggesting that they are activated (25). Treatment of *Sftpd*$^{-/-}$ mice with ozone resulted in significant increases in macrophages in the lung, as reflected by inflammation scores and BAL cell numbers, as well as by BAL protein and NOx concentrations and chemotactic activity. These results are novel and indicate that oxidative stress and macrophage localization and activation in the lung after ozone exposure are prolonged in *Sftpd*$^{-/-}$ mice. Ozone-induced lung injury is characterized by the disruption of epithelial tight junctions and increases in blood/air barrier permeability, resulting in increases in BAL protein content (34, 35). Our data demonstrate that persistent pulmonary macrophage inflammation, resulting from a loss of *Sftpd*, also results in prolonged sensitivity of the mice to the cytotoxic effects of ozone.

iNOS and COX-2 are key enzymes in the generation of the cytotoxic and proinflammatory RNS and eicosanoids implicated in lung injury induced by inhaled irritants (3, 27). In previous studies, we reported that ozone inhalation resulted in increased expression of iNOS and COX-2 in lung macrophages and Type II cells, a response that was evident 0–48 hours after exposure (18, 19, 36). The present experiments demonstrate

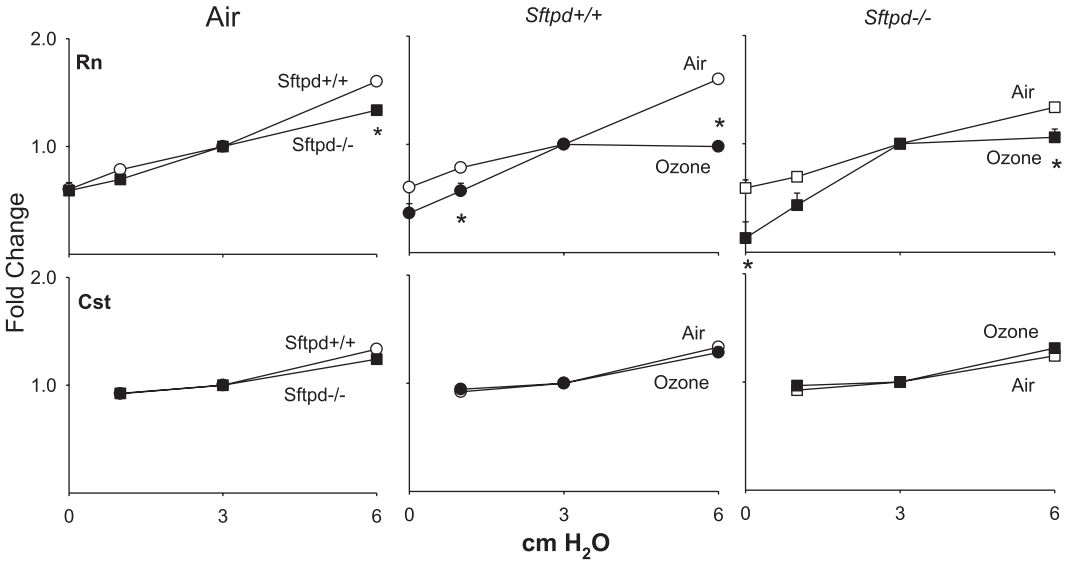

Figure 4. Effects of ozone inhalation on central airway resistance (Rn) and static compliance (Cst) in *Sftpd*$^{+/+}$ and *Sftpd*$^{-/-}$ mice. Lung function was measured 72 hours after exposure of *Sftpd*$^{+/+}$ (*circles*) and *Sftpd*$^{-/-}$ (*squares*) mice to air (*open symbols*) or ozone (*solid symbols*). Lungs were subjected to increasing positive end-expiratory pressure (PEEP). *Top row*: For Rn, impedance spectra were measured using the forced oscillation technique. Results were analyzed using the constant phase model. *Bottom row*: Cst was calculated from pressure–volume loops. Measurements were performed in triplicate at each PEEP. For each sample at each PEEP, Rn and Cst values were normalized to PEEP = 3, the physiological pressure for mice. Each point represents the mean ± SEM of three experiments (n = 4–6 mice/treatment group/experiment; n = 12–27 mice/group total). Data were analyzed by two-way ANOVA and a nonpaired, two-tailed Student t test. *Significantly different ($P \leq 0.05$) from air-exposed or *Sftpd*$^{+/+}$ control mice.

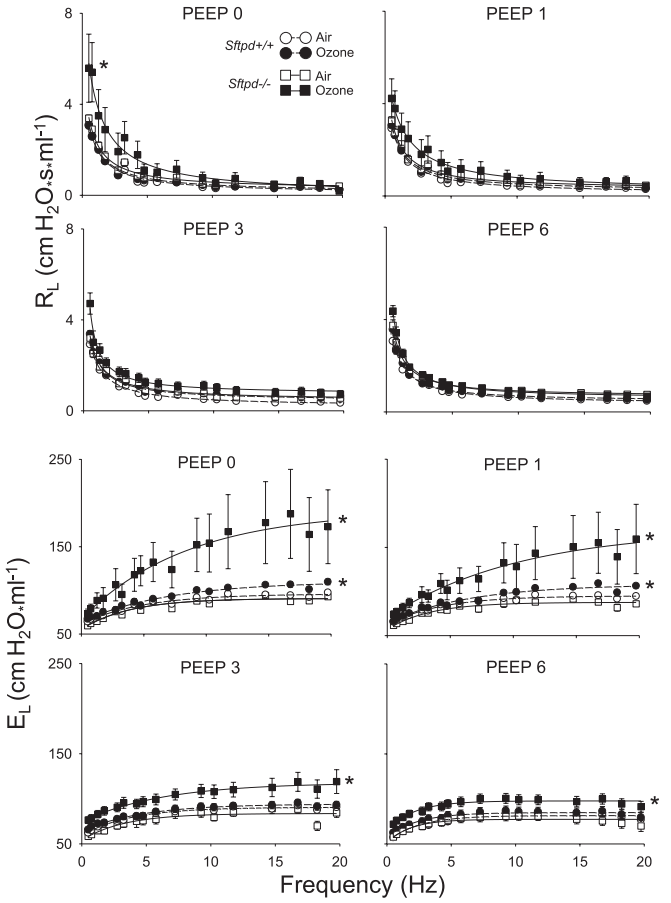

Figure 5. Effects of ozone inhalation on resistance spectra curves (R_L) and elastance spectra curves (E_L) in *Sftpd*$^{+/+}$ and *Sftpd*$^{-/-}$ mice. Lung function was measured 72 hours after exposure of *Sftpd*$^{+/+}$ and *Sftpd*$^{-/-}$ mice to air or ozone. Lungs were subjected to increasing PEEP. Impedance spectra were generated using the forced oscillation technique. Resistance and elastance spectra were then derived from input impedance data. Measurements were performed in triplicate at each PEEP. Each point represents the mean ± SEM of three experiments ($n = 4$–6 mice/treatment group/experiment; $n = 12$–27 mice/group total). Data were analyzed by nonlinear regression. *Significantly different ($P \leq 0.05$) from air-exposed control mice.

that although ozone-induced increases in Type II cell expression of COX-2 persisted for at least 72 hours in *Sftpd*$^{+/+}$ mice, macrophage expression of iNOS was transient. These findings are consistent with the resolution of macrophage-mediated inflammation at this time (18). In *Sftpd*$^{-/-}$ mice, however, macrophage expression of iNOS remained elevated above control levels for at least 72 hours after ozone inhalation. These data suggest the persistence of a proinflammatory macrophage phenotype in *Sftpd*$^{-/-}$ mice. Earlier work reported on increased constitutive expression of iNOS in macrophages and alterations in nitric oxide metabolites in the lungs of *Sftpd*$^{-/-}$ mice (17). Moreover, treatment of these mice with an iNOS inhibitor attenuated the inflammatory responses associated with a loss of *Sftpd* (37). The favoring of proinflammatory macrophage activation in the lungs of *Sftpd*$^{-/-}$ mice, which occurs as a consequence of excessive iNOS activity, may lead to a hypersusceptible state, such that ozone-mediated injury and oxidative stress are prolonged. Surprisingly, BAL NOx concentrations were similar in ozone-treated *Sftpd*$^{+/+}$ and *Sftpd*$^{-/-}$ mice. These results most likely reflects the fact that NOx is only a measure of the extracellular pool of nitric oxide metabolites. Notably, we observed that ozone-induced increases in Type II cell COX-2 also remained elevated above air-exposed control levels in *Sftpd*$^{-/-}$ mice 72 hours after ozone exposure. These data provide additional support for the role of Type II cells in the inflammatory response to ozone (36).

Baseline central airway and parenchymal mechanics have been reported to be altered in *Sftpd*$^{-/-}$ mice, compared with *Sftpd*$^{+/+}$ mice (38). Similarly, we observed alterations in central airway pulmonary mechanics in *Sftpd*$^{-/-}$ mice relative to *Sftpd*$^{+/+}$ mice, as measured by increases in R, Rn, and Cst (39). In addition, at all PEEPs measured, R_L was greater at high frequencies, suggesting that persistent pulmonary inflammation in *Sftpd*$^{-/-}$ mice leads to alterations in central airway mechanics. Our findings that these alterations are similar to the effects of ozone in *Sftpd*$^{+/+}$ mice provide support for this conclusion. We also found that loss of *Sftpd* altered the elastic recoil properties of the lung parenchyma, and caused increases in heterogeneous ventilation, airway resistance, and lung stiffness. In contrast to our findings, decreases in the elastic recoil of lung parenchyma were previously described in *Sftpd*$^{-/-}$ mice (38). Differences between our findings and previous results may be attributable to differences in the ages of mice analyzed.

Because of preexisting macrophage inflammation, we speculated that ozone-induced alterations in pulmonary mechanics would be more extensive in *Sftpd*$^{-/-}$ mice, compared with ozone-exposed *Sftpd*$^{+/+}$ mice, and this was the case. Thus, in *Sftpd*$^{-/-}$ mice, ozone inhalation resulted in alterations not only in airway mechanics, but also in the parenchymal integrity of

TABLE 2. EFFECTS OF OZONE ON R_L AND E_L SPECTRA IN *SFTPD*$^{+/+}$ AND *SFTPD*$^{-/-}$ MICE

		Sftpd$^{+/+}$		*Sftpd*$^{-/-}$	
	PEEP	Air	Ozone	Air	Ozone
a	0	3.39 ± 0.11	3.62 ± 0.19	3.69 ± 0.16	8.71 ± 3.41
	1	3.50 ± 0.05	3.53 ± 0.19	3.52 ± 0.32	8.09 ± 3.76
	3	3.20 ± 0.07	2.91 ± 0.22	3.32 ± 0.20	3.12 ± 0.71
	6	3.20 ± 0.13	2.59 ± 0.18	2.89 ± 0.19	3.16 ± 0.25
b	0	0.08 ± 0.01	0.13 ± 0.04	0.24 ± 0.04*	−0.06 ± 0.09†
	1	0.10 ± 0.02	0.20 ± 0.04†	0.29 ± 0.04*	0.13 ± 0.04†
	3	0.19 ± 0.01	0.43 ± 0.02†	0.45 ± 0.01*	0.73 ± 0.17
	6	0.34 ± 0.01	0.45 ± 0.01	0.66 ± 0.01*	0.57 ± 0.06
c	0	0.58 ± 0.03	0.70 ± 0.06	0.62 ± 0.05	0.76 ± 0.19
	1	0.67 ± 0.03	0.68 ± 0.04	0.60 ± 0.04	1.05 ± 0.33
	3	0.61 ± 0.01	0.45 ± 0.05	0.67 ± 0.13	0.31 ± 0.16
	6	0.58 ± 0.02	0.30 ± 0.02†	0.37 ± 0.03*	0.29 ± 0.03
E_0	0	61.36 ± 1.21	63.75 ± 1.35	54.90 ± 0.96*	66.46 ± 4.92
	1	62.08 ± 1.11	64.04 ± 1.22	56.62 ± 1.95*	69.26 ± 2.40†
	3	59.18 ± 1.31	64.04 ± 2.43	53.66 ± 2.15	73.88 ± 4.20†
	6	52.45 ± 1.35	57.37 ± 3.41	51.19 ± 2.89	65.24 ± 3.25†
ΔE	0	34.57 ± 0.85	46.92 ± 2.75†	36.55 ± 0.83	130.54 ± 56.58†
	1	32.99 ± 0.65	44.60 ± 1.59†	31.16 ± 1.75	115.18 ± 60.07†
	3	31.43 ± 0.77	30.61 ± 1.73	30.12 ± 2.69	57.01 ± 19.96
	6	29.02 ± 0.81	27.52 ± 1.92	26.18 ± 2.29	32.59 ± 2.46
β	0	0.20 ± 0.00	0.15 ± 0.02†	0.27 ± 0.05	0.18 ± 0.03†
	1	0.24 ± 0.01	0.16 ± 0.02†	0.30 ± 0.03	0.14 ± 0.03†
	3	0.27 ± 0.01	0.22 ± 0.02	0.30 ± 0.03	0.21 ± 0.04
	6	0.41 ± 0.01	0.44 ± 0.03	0.56 ± 0.05*	0.48 ± 0.03

Definition of abbreviations: a, b, and c are parameters of R_L; a and c reflect R_L at low frequencies; b reflects R_L at high frequencies. E_0, ΔE, and β are parameters of E_L; E_L, elastance spectra curve; R_L, resistance spectra curve.

E_0 represents E_L at 0 Hz. ΔE reflects the magnitude of E_L, and β the rate of E_L change with frequency. Lung function was measured 72 hours after exposure of *Sftpd*$^{+/+}$ and *Sftpd*$^{-/-}$ mice to air or ozone. Each measurement was performed in triplicate. Values represent the means ± SEM of three experiments ($n = 4$–6 mice/treatment group/experiment; $n = 12$–18 mice/group total). Data were analyzed by two-way ANOVA.

* Significantly different ($P < 0.05$) from *Sftpd*$^{+/+}$ mice.

† Significantly different ($P < 0.05$) from air-exposed control mice.

the already compromised lungs. In the lungs of *Sftpd*$^{-/-}$ mice, an accumulation of inflammatory macrophages occurred, which increased after ozone exposure, along with pronounced lipoproteinosis. This buildup of inflammatory material may cause a stiffening of the lung, with a consequent increase in inherent tissue elastance. This idea is supported by our observation that in the derecruited lung, ozone exposure resulted in a dramatic increase in E_L, a change that was frequency-dependent and delayed, compared with air-exposed *Sftpd*$^{-/-}$ mice. Moreover, constant phase model analysis revealed increased baseline tissue elastance, which is consistent with a stiffening effect on parenchymal mechanics and indicative of restrictive lung injury. This increased baseline tissue elastance was not observed in ozone-exposed *Sftpd*$^{+/+}$ mice, suggesting that Sftpd is important in maintaining the elastic properties of the lung. Increases in both R_L and E_L spectra at low frequencies suggest that in *Sftpd*$^{-/-}$ mice, ozone exposure results in heterogeneous changes in lung function (40). The observation that these changes were ameliorated as PEEP increased indicates that ozone exposure, like a loss of *Sftpd*, affects parenchymal tethering, which could result in small airway collapse. Functionally, *Sftpd*$^{-/-}$ mice appear similar to ozone-injured *Sftpd*$^{+/+}$ mice, with an apparent loss of parenchymal integrity resulting in derecruitment and a loss of airway tethering. Taken together, these results indicate that lung function is significantly altered by both a loss of *Sftpd* and by ozone exposure, and that an interaction between these proinflammatory stimuli occurs. These results support findings in other models of lung injury that Sftpd is important in maintaining normal lung functioning (38, 41–43).

In previous studies, Kierstein and colleagues (44) reported increased numbers of neutrophils in BAL fluid 12–48 hours after exposure of *Sftpd*$^{-/-}$ mice to ozone. However, the effects of ozone on macrophage accumulation and activation in the lung were not assessed. Lung injury, oxidative stress, and pulmonary mechanics were also not evaluated. Thus, the results presented here, demonstrating sustained lung injury, oxidative stress, and macrophage activation, and exacerbated alterations in pulmonary mechanics, are novel. Also unique to the present study is the use of a constant phase model of lung function to assess alterations in central airway mechanics, and our analysis of resistance and elastance spectra at various levels of PEEP. This analysis revealed the importance of parenchymal injury in mediating changes in lung function. Because polymorphisms in *Sftpd* have been associated with the development of COPD (45), this study highlights the importance of understanding the role of persistent inflammation caused by the loss of this protein on the response of susceptible populations to ozone exposure. We emphasize that in the present experiments, *Sftpd*$^{-/-}$ mice were used as a model of persistent pulmonary macrophage inflammation. At present, it remains unclear whether the absence of *Sftpd* or underlying inflammation is responsible for the observed differences in ozone responses between *Sftpd*$^{+/+}$ and *Sftpd*$^{-/-}$ mice. Further studies using an experimental model of conditional loss of *Sftpd* would enable an assessment of the specific effects of deficiency in this protein on lung responses to ozone.

Author disclosures are available with the text of this article at www.atsjournals.org.

References

1. Ciencewicki J, Trivedi S, Kleeberger SR. Oxidants and the pathogenesis of lung diseases. *J Allergy Clin Immunol* 2008;122:456–468.
2. Al-Hegelan M, Tighe RM, Castillo C, Hollingsworth JW. Ambient ozone and pulmonary innate immunity. *Immunol Res* 2011;49:173–191.
3. Laskin DL, Sunil VR, Gardner CR, Laskin JD. Macrophages and tissue injury: agents of defense or destruction? *Annu Rev Pharmacol Toxicol* 2011;10:267–288.
4. Que LG, Stiles JV, Sundy JS, Foster WM. Pulmonary function, bronchial reactivity, and epithelial permeability are response phenotypes to ozone and develop differentially in healthy humans. *J Appl Physiol* 2011;111:679–687.
5. Foster WM, Brown RH, Macri K, Mitchell CS. Bronchial reactivity of healthy subjects: 18–20 h postexposure to ozone. *J Appl Physiol* 2000; 89:1804–1810.
6. Kim BJ, Kwon JW, Seo JH, Kim HB, Lee SY, Park KS, Kim HC, Leem JH, Sakong J, Kim SY, *et al*. Association of ozone exposure with asthma, allergic rhinitis, and allergic sensitization. *Ann Allergy Asthma Immunol* 2011;107:214–219.
7. Desqueyroux H, Pujet JC, Prosper M, Le Moullec Y, Momas I. Effects of air pollution on adults with chronic obstructive pulmonary disease. *Arch Environ Health* 2002;57:554–560.
8. Zanobetti A, Schwartz J. Ozone and survival in four cohorts with potentially predisposing diseases. *Am J Respir Crit Care Med* 2011;184: 836–841.
9. Gilmour MI, Park P, Selgrade MK. Ozone-enhanced pulmonary infection with *Streptococcus zooepidemicus* in mice: the role of alveolar macrophage function and capsular virulence factors. *Am Rev Respir Dis* 1993;147:753–760.
10. Kierstein S, Krytska K, Sharma S, Armani Y, Salmon M, Panettieri RA, Zangrilli J, Haczku A. Ozone inhalation induces exacerbation of eosinophilic airway inflammation and hyperresponsiveness in allergen-sensitized mice. *Allergy* 2008;63:438–446.
11. Rivera-Sanchez YM, Johnston RA, Schwartzman IN, Valone J, Silverman ES, Fredberg JJ, Shore SA. Differential effects of ozone on airway and tissue mechanics in obese mice. *J Appl Physiol* 2004;96: 2200–2206.
12. Crouch E, Wright J. Surfactant proteins A and D and pulmonary host defense. *Annu Rev Physiol* 2001;63:521–554.
13. Haczku A. Protective role of the lung collectins surfactant protein A and surfactant protein D in airway inflammation. *J Allergy Clin Immunol* 2008;122:861–879.
14. Gardai SJ, Xiao YQ, Dickinson M, Nick JA, Voelker DR, Greene KE, Henson PM. By binding SIRPα or calreticulin/CD91, lung collectins act as dual function surveillance molecules to suppress or enhance inflammation. *Cell* 2003;115:13–23.
15. Guo CJ, Atochina-Vasserman EN, Abramova E, Foley JP, Zaman A, Crouch E, Beers MF, Savani RC, Gow AJ. S-nitrosylation of surfactant protein–D controls inflammatory function. *PLoS Biol* 2008;6: 2414–2423.
16. Yoshida M, Korhagen TR, Whitsett JA. Surfactant protein D regulates NF-kappa B and matrix metalloproteinase production in alveolar macrophages via oxidant-sensitive pathways. *J Immunol* 2001;166: 7514–7519.
17. Atochina EN, Beers MF, Hawgood S, Poulain F, Davis C, Fusaro T, Gow AJ. Surfactant protein–D, a mediator of innate lung immunity, alters the products of nitric oxide metabolism. *Am J Respir Cell Mol Biol* 2004;30:271–279.
18. Fakhrzadeh L, Laskin JD, Laskin DL. Deficiency in inducible nitric oxide synthase protects mice from ozone-induced lung inflammation and tissue injury. *Am J Respir Cell Mol Biol* 2002;26:413–419.
19. Fakhrzadeh L, Laskin JD, Laskin DL. Ozone-induced production of nitric oxide and TNF-α and tissue injury are dependent on NF-κB p50. *Am J Physiol Lung Cell Mol Physiol* 2004;287:L279–L285.
20. Botas C, Poulain F, Akiyama J, Brown C, Allen L, Groerke J, Clements J, Carlson E, Gillespie AM, Epstein C, *et al*. Altered surfactant homeostasis and alveolar Type II cell morphology in mice lacking surfactant protein D. *Proc Natl Acad Sci USA* 1998;95:11869–11874.
21. Rudmann DG, Preston AM, Moore MW, Beck JM. Susceptibility to *Pneumocystis carinii* in mice is dependent on simultaneous deletion of IFN-γ and Type 1 and 2 TNF receptor genes. *J Immunol* 1998;161: 360–366.
22. Sunil VR, Patel-Vayas K, Shen J, Gow AJ, Laskin JD, Laskin DL. Role of TNFR1 in lung injury and altered lung function induced by the model sulfur mustard vesicant, 2–chloroethyl ethyl sulfide. *Toxicol Appl Pharmacol* 2011;250:245–255.
23. Ito S, Bartolak-Suki E, Shipley JM, Parameswaran H, Majumdar A, Suki B. Early emphysema in the tight skin and pallid mice: roles of mirofibril-associated glycoproteins, collagen, and mechanical forces. *Am J Respir Cell Mol Biol* 2006;34:688–694.

24. Hantos Z, Daroczy B, Suki B, Nagy S, Fredburg JJ. Imput impedance and peripheral inhomogeneity of dog lungs. *J Appl Physiol* 1992;72: 168–178.
25. Wert SE, Yoshida M, LeVine AM, Ikegami M, Jones T, Ross GF, Fisher JH, Korfhagen TR, Whitsett JA. Increased metalloproteinase activity, oxidant production and emphysema in surfactant protein D gene-inactivated mice. *Proc Natl Acad Sci USA* 2000;97:5972–5977.
26. Laskin JD, Heck DE, Laskin DL. Nitric oxide pathways in toxic responses. In: Ballantyne B, Marrs T, Syversen T, editors. General and applied toxicology. Chichester, UK: Wiley-Blackwell; 2010. pp. 425–438.
27. Park GY, Christman JW. Involvement of cyclooxygenase-2 and prostaglandins in the molecular pathogenesis of inflammatory lung diseases. *Am J Physiol Lung Cell Mol Physiol* 2006;290:L797–L805.
28. Munder M, Eichmann K, Modolell M. Alternative metabolic states in murine macrophages reflected by the nitric oxide synthase/arginase balance: competitive regulation by $CD4^+$ T cells correlates with Th1/Th2 phenotype. *J Immunol* 1998;160:5347–5354.
29. Stout R, Jiang C, Matta B, Illya T, Watkins S, Suttles J. Macrophages sequentially change their functional phenotype in response to changes in microevnironmental influences. *J Immunol* 2005;175:342–349.
30. Massa CB, Allen GB, Bates JH. Modeling the dynamics of recruitment and derecruitment in mice with acute lung injury. *J Appl Physiol* 2008; 105:1813–1821.
31. Kaczka DW, Lutchen KR, Hantos Z. Emergent behavior of regional heterogeneity in the lung and its effects on respiratory impedance. *J Appl Physiol* 2011;110:1473–1481.
32. Hollingsworth JW, Maruoka S, Li Z, Potts EN, Brass DM, Garantziotis S, Fong A, Foster WM, Schwartz DA. Ambient ozone primes pulmonary innate immunity in mice. *J Immunol* 2007;179:4367–4375.
33. Petak F, Hantos Z, Adamicza A, Daroczy B. Partitioning of pulmonary impedance: modeling vs. alveolar capsule approach. *J Appl Physiol* 1993;75:513–521.
34. Foster WM, Stetkiewicz PT. Regional clearance of solute from the respiratory epithelia: 18–20 h post exposure to ozone. *J Appl Physiol* 1996;81:1143–1149.
35. Bhalla DK. Ozone induced lung inflammation and mucosal barrier disruption: toxicology, mechanisms, and implications. *J Toxicol Environ Health B Crit Rev* 1999;2:31–86.
36. Punjabi CJ, Laskin JD, Pendino KJ, Goller NL, Durham SK, Laskin DL. Production of nitric oxide by rat Type II pneumocytes: increased expression of inducible nitric oxide synthase following inhalation of a pulmonary irritant. *Am J Respir Cell Mol Biol* 1994;11:165–172.
37. Atochina-Vasserman EN, Beers MF, Kadire H, Tomer Y, Inch A, Scott P, Guo CJ, Gow AJ. Selective inhibition of inducible NO synthase activity *in vivo* reverses inflammatory abnormalities in surfactant protein D–deficient mice. *J Immunol* 2007;179:8090–8097.
38. Collins RA, Ikegami M, Korfhagen TR, Whitsett JA, Sly PD. *In vivo* measurements of changes in respiratory mechanics with age in mice deficient in surfactant protein D. *Pediatr Res* 2003;53:463–467.
39. Vanoirbeek JA, Rinaldi M, De Vooght V, Haenen S, Bobic S, Gayen-Ramirez G, Hoet PH, Verbeken E, Decramer M, Nemery B, *et al*. Noninvasive and invasive pulmonary function in mouse models of obstructive and restrictive respiratory diseases. *Am J Respir Cell Mol Biol* 2010;42:96–104.
40. Lutchen KR, Gillis H. Relationship between heterogeneous changes in airway morphology and lung resistance and elastance. *J Appl Physiol* 1997;83:1192–1201.
41. Takeda K, Miyahara N, Rha YH, Taube C, Yang ES, Joetham A, Kodama T, Balhorn AM, Dakhama A, Duez C, *et al*. Surfactant protein D regulates airway function and allergic inflammation through modulation of macrophage function. *Am J Respir Crit Care Med* 2003;168:783–789.
42. Atochina EN, Beers MR, Tomer Y, Scanlon ST, Russo SJ, Panettieri RA Jr., Haczku A. Attenuated allergic airway hyperresponsiveness in C57BL/6 mice is associated with enhanced surfactant protein (SP)–D production following allergic sensitization. *Respir Res* 2003;8:15–27.
43. Erpenjeck VJ, Ziegert M, Cavalet-Blanco D, Martin C, Baelder R, Glaab T, Braun A, Steinhilber W, Luettig B, Uhlig S, *et al*. Surfactant protein D inhibits early airway response in *Aspergillus fumigatus*–sensitized mice. *Clin Exp Allergy* 2006;36:930–940.
44. Kierstein S, Poulain FR, Cao Y, Grous M, Mathias R, Kierstein G, Beers MF, Salmon M, Panettieri RA, Haczku A. Susceptibility to ozone-induced airway inflammation is associated with decreased levels of surfactant protein D. *Respir Res* 2006;7:85.
45. Kishore U, Bernal AL, Kamran MF, Saxena S, Singh M, Sarma PU, Madan T, Chakraborty T. Surfactant proteins SP-A and SP-D in human health and disease. *Arch Immunol Ther Exp* 2005;53:399–417.